A New Approach to Response Surface Development for Detailed Gas-Phase and Surface Reaction Kinetic Model Optimization

SCOTT G. DAVIS,[1] ASHISH B. MHADESHWAR,[2,3] DIONISIOS G. VLACHOS,[2,3] HAI WANG[1,3]

[1]*Department of Mechanical Engineering, University of Delaware, Newark, Delaware* 19716
[2]*Department of Chemical Engineering, University of Delaware, Newark, Delaware* 19716
[3]*Center for Catalytic Science and Technology, University of Delaware, Newark, Delaware* 19716

Received 1 October 2002; accepted 29 September 2003

DOI 10.1002/kin.10177

ABSTRACT: We propose a new method for constructing kinetic response surfaces used in the development and optimization of gas-phase and surface reaction kinetic models. The method, termed as the sensitivity analysis based (SAB) method, is based on a multivariate Taylor expansion of model response with respect to model parameters, neglecting terms higher than the second order. The expansion coefficients are obtained by a first-order local sensitivity analysis. Tests are made for gas-phase combustion reaction models. The results show that the response surface obtained with the SAB method is as accurate as the factorial design method traditionally used in reaction model optimization. The SAB method, however, presents significant computational savings compared to factorial design. The effect of including the partial and full third order terms was also examined and discussed. The SAB method is applied to optimization of a relatively complex surface reaction mechanism where large uncertainty in rate parameters exists. The example chosen is laser-induced fluorescence signal of OH desorption from a platinum foil in the water/oxygen reaction at low pressures. We introduce an iterative solution mapping and optimization approach for improved accuracy. © 2003 Wiley Periodicals, Inc. Int J Chem Kinet 36: 94–106, 2004

Correspondence to: Hai Wang; e-mail: hwang@me.udel.edu.
Present address of Scott G. Davis: Exponent, Inc., 21 Strathmore Road, Natick, MA 01760.
Contract grant sponsor: Air Force Office of Scientific Research.
Contract grant number: F496200110144.
Contract grant sponsor: National Science Foundation.
Contract grant number: CTS9874768.
Contract grant sponsor: U.S. Department of Energy.
Contract grant number: DE-FC26-00NT41027.
© 2003 Wiley Periodicals, Inc.

INTRODUCTION

It has become increasingly feasible to carry out numerical simulations of complex gas-phase, surface, and gas-surface reacting flow problems using detailed chemical kinetic models. These models are composed of elementary reactions and their associated rate parameters. An accurate prediction of a wide range of reacting flow problems relies heavily on the availability of accurate rate parameters. For gas-phase combustion of hydrocarbons, there are a wealth of fundamental kinetic data and reaction rate parameters measured under chemical isolation. Even in this best-case scenario, however, models consisting of individually measured rate parameters may not and usually do not predict a range of reacting flow data with desirable accuracy [1]. The reason behind this unsatisfactory situation is obvious. When reactions and their rate parameters are evaluated and placed in a kinetic model, the inherent uncertainties of rate parameters form an uncertainty hypercube. Without the constraints of combustion response data, each point within the hypercube is probable and allowable. With the constraints, the hypercube of uncertainty "shrinks" to a surface of finite thickness. Regardless of how carefully a kinetic model is compiled and how comprehensive it is, it represents just a random point on this uncertainty surface.

In other cases like gas-surface reaction processes, obtaining accurate rate parameters is often difficult. Rate expressions in catalytic reactor modeling have generally followed a reductionistic approach [2], and even nowadays, empirical rate expressions are common. Using the microkinetic analysis approach [3], elementary reaction mechanisms can be developed without relying on a rate-determining step (RDS). A key issue in rendering the microkinetic analysis powerful is estimation of rate parameters of these elementary reactions such as preexponential factors, sticking coefficients, and activation energies along with their surface coverage dependence.

Regardless of how accurate the initial rate estimates are, model adjustments are almost always necessary. These adjustments are customarily accomplished by tuning rate parameters, often in an ad hoc manner, within their physically allowable bounds or the uncertainty bounds. This approach amounts to an effort to shift model parameters from their nominal values, which represent the initial random point in the uncertainty hyperspace, to a point that would better predict a given set of experimental data. Because the dimensionality of the uncertainty space is usually very large and the selection of the initial point is often arbitrary, a model validated under certain conditions may not predict the experiments under other conditions. To bring a model to a truly predictive level under a wide range of conditions, it is necessary to carry out systematic optimization of the reaction rate parameters against a wide range of experimental data.

An optimization approach has been developed [1,4] and applied to gas-phase combustion reaction models [1,5–7] and surface reaction models of H_2 and CO oxidation on platinum (Pt) [8,9]. In this method, a trial reaction model is first compiled. A set of experimental data is selected as optimization targets. Since not all rate parameters equally affect a given experimental response, a sensitivity analysis is conducted to determine a list of active rate parameters, which usually number in several dozens for typical combustion problems. Then the optimization is carried out by minimizing a least-squares objective function, e.g., $\sum_i [1 - \eta_i(\mathbf{x})/\eta_{\text{expt},i}]^2$, with respect to active parameter $\mathbf{x}$, where $\eta_i(\mathbf{x})$ is the model response of the ith experiment, and $\eta_{\text{expt},i}$ is the value of that experiment.

Because the evaluation of $\eta_i(\mathbf{x})$ requires numerical solutions of coupled differential equations, it is prohibitive to carry out a minimization procedure by direct solution of these equations. To solve this problem, a solution mapping technique was proposed [4]. In this method, a kinetic response surface is constructed, which expresses the response value as a function of model parameters by a second- or third-order polynomial,

$$\eta = a_0 + \sum_i^L a_i x_i + \sum_i^L \sum_{j \geq i}^L a_{ij} x_i x_j + \sum_i^L \sum_{j \geq i}^L \sum_{k \geq j}^L a_{ijk} x_i x_j x_k \tag{1}$$

where L is the number of active rate parameters in that target, and x_i is the ith rate parameter k_i normalized by its uncertainty factor f_i [4],

$$x_i = \frac{\ln(k_i/k_{i,0})}{\ln f_i} \tag{2}$$

Here $k_{i,0}$ is the nominal rate parameter of reaction i. The upper and lower bounds of uncertainty correspond to $x_i = +1$ and -1, respectively, and the nominal rate parameter is given by $x_i = 0$. Obviously, a kinetic response surface is useful not only for model optimization, but also for a quick but quantitative examination of the influences of model parameters on model predictions.

In Eq. (1), the coefficients a are traditionally obtained by regression of a factorial test [10]. This method has been shown to provide reliable and accurate response surfaces [1]. Its use, however, may become prohibitively expensive when L is large. For complex

systems the development of response surfaces for combustion properties such as the laminar flame speed can be a very time demanding task. A recent example can be found in the work of Qin et al. [7], where 539 numerical flame solutions were required to determine the response surface of 13 active parameters for the flame speed of propane; and 12 such flame response surfaces were needed for optimization.

The objective of the present work is to develop an efficient and accurate response surface method. This sensitivity-analysis based method, hereafter referred to as the SAB method, is based on a multivariate expansion of model response with respect to model parameters. The coefficients of the response surface are determined by sensitivity analysis. In the first application, the SAB method is tested for problems of gas-phase combustion, including the laminar flame speed and species concentration in a burner stabilized flame. The second application we present here comes from catalysis. The specific example is the modeling of laser-induced fluorescence (LIF) signal of OH desorption from a Pt foil in the water/oxygen reaction at low pressures. An important difference of catalytic kinetic modeling from gas-phase combustion lies in the large uncertainty in kinetic parameters of surface reactions. An iterative surface solution mapping/optimization methodology is introduced and tested. The iterative procedure further exemplifies the utility of the SAB method developed herein.

OVERVIEW OF THEORY

Traditionally, a response surface is obtained by computing response values at a set of 2^L factorial design points in the uncertainty hypercube, followed by a regression analysis of the response values [10]. As demonstrated in Fig. 1a for a 3-active parameter problem, the full 2^L factorial design consists of the corner points of the cube (filled circles), the origin (open circle), and two "star" points on each major axis [4].

A full 2^L factorial design requires $2^L + 2L + 1$ numerical experiments, and is therefore computationally costly for systems with large L values. In practice a 2^{L-M} fractional factorial design is often used. Here M cannot be very large as the accuracy decreases rapidly as M increases. Taking the gas-phase combustion of propane as an example [7], the dimension of the response surface was $L = 13$. Setting M equal to 4 gives $2^{13-4} + 2 \times 13 + 1 = 539$ solutions of differential equations in order to construct the response surface.

An alternative approach is to view the response surface as a multivariate Taylor expansion of $\eta(\mathbf{x})$ about $\mathbf{x} = \mathbf{0}$, where $\mathbf{x} = \{x_1, x_2, \ldots, x_L\}$:

$$\eta(\mathbf{x}) = \eta(0) + \sum_i^L \left.\frac{\partial \eta}{\partial x_i}\right|_0 x_i + \frac{1}{2}\sum_i^L \left.\frac{\partial^2 \eta}{\partial x_i^2}\right|_0 x_i^2 + \sum_i^L \sum_{j>i}^L \left.\frac{\partial^2 \eta}{\partial x_i \partial x_j}\right|_0 x_i x_j + \frac{1}{6}\sum_i^L \left.\frac{\partial^3 \eta}{\partial x_i^3}\right|_0 x_i^3 + \frac{1}{2}\sum_i^L \sum_{j\neq i}^L \left.\frac{\partial^3 \eta}{\partial x_i^2 \partial x_j}\right|_0 x_i^2 x_j + \sum_i^L \sum_{j>i}^L \sum_{k>j}^L \left.\frac{\partial^3 \eta}{\partial x_i \partial x_j \partial x_k}\right|_0 x_i x_j x_k + \cdots \quad (3)$$

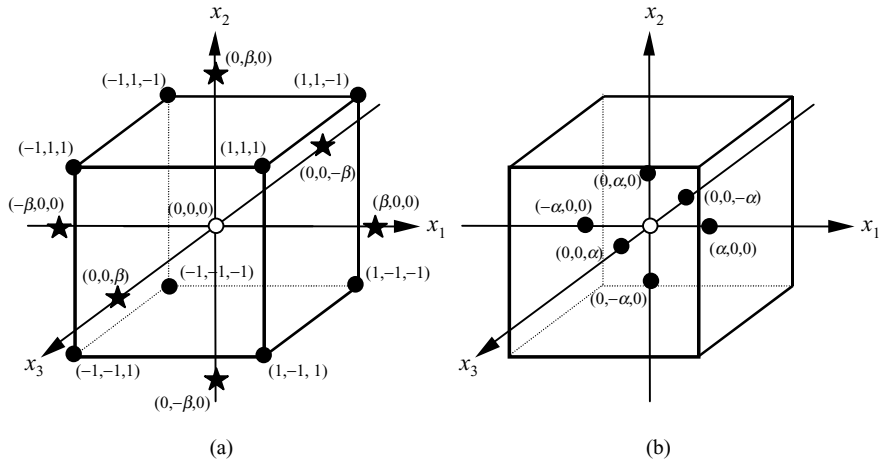

Figure 1 Three dimensional uncertainty hypercube of normalized rate parameters, illustrating the methods of factorial design (a) and the proposed sensitivity analysis-based (SAB) method (b). In (a), the filled circles represent the corner points of the hypercube; the open symbol is the center; the "stars" are the star points (see text). In (b), the filled and open symbols represent the $2 \times 3 + 1$ sensitivity computations required to construct the response surface.

The SAB method proposed herein utilizes the fact that the first derivative, $\partial\eta/\partial x_i|_0$, is related to the first-order sensitivity coefficient, s_i,

$$\left.\frac{\partial \eta}{\partial x_i}\right|_0 = \eta(0) s_i \ln f_i \tag{4}$$

where $s_i = \partial \ln \eta(0) / \partial \ln k_i$ and $\eta(0)$ is the nominal response value. The second-order derivatives are the second-order sensitivity coefficients and can be obtained by finite differencing the local first-order sensitivity coefficients.

It can be shown that the SAB method requires only $2L + 1$ local sensitivity calculations (Fig. 1b) to obtain all first- and second-order coefficients. These calculations will require slightly more computational time at each point. Overall, the SAB method presents significant computational savings compared to the $2^{L-M} + 2L + 1$ computations by the fractional factorial design, as will be demonstrated in a later section. Further computational savings arise from the fact that solutions of the corner and star points in the factorial method are often very different from that at the center point. Hence the solution of these points is often subject to divergence during the Newton procedure when the center-point solution is used as the initial guess. The SAB method, on the other hand, only varies one variable at a time and those points lie within the parameter "cube," resulting in solutions that are often not so different from the nominal one. For this reason, convergence of the flame solution for sensitivity calculation is usually rapid. In addition, the $2L + 1$ local sensitivity calculations also yield the x_i^3 and $x_i^2 x_j$ terms without extra computations. These terms can improve the accuracy of highly curved response surfaces, as will be discussed later.

NUMERICAL METHODOLOGY

The Sensitivity Analysis-Based (SAB) Method

We carry out sensitivity coefficient computations (with respect to L active rate parameters) for $2L + 1$ points, i.e., two points for each active parameter along its major axis and the center point, as shown in Fig. 1b. The 0th order coefficient is simply the nominal response value, $a_0 = \eta(0)$. The first-order coefficients of Eq. (1) can be obtained from a local sensitivity analysis about the nominal rate parameter vector. Here they are expressed in a finite difference form as

$$a_i = \frac{\eta[\mathbf{x}(\alpha)_i] - \eta[\mathbf{x}(-\alpha)_i]}{2\alpha} \quad (i = 1, 2, \ldots, L) \tag{5}$$

where $\mathbf{x}(\alpha)_i$ denotes a vector of normalized rate parameters, whose elements are equal to 0 with the exception of the ith parameter, which is perturbed by α, $\mathbf{x}(\pm\alpha)_i = [0, 0, \ldots, x_i = \pm\alpha, \ldots, 0]$. The second-order coefficients are determined by finite differencing the first-order sensitivity coefficients s,

$$a_{ii} = \frac{s_{i,i} - s_{-i,i}}{4\alpha} a_0 \ln f_i \tag{6a}$$

$$a_{ij} = \frac{[(s_{i,j} - s_{-i,j}) \ln f_j + (s_{j,i} - s_{-j,i}) \ln f_i]}{4\alpha} a_0 \quad (i \neq j) \tag{6b}$$

where $s_{i,j}$ is the sensitivity coefficient with respected to the jth rate parameter k_j, calculated for the rate parameter vector $\mathbf{x}(\alpha)_i$, $s_{\pm i,j} = \partial \ln \eta[\mathbf{x}(\pm\alpha)_i] / \partial \ln k_j$. The third-order coefficients a_{iii} and a_{iij} may be determined from the first derivatives as

$$a_{iii} = \frac{s_{i,i} - 2s_{0,i} + s_{-i,i}}{6\alpha^2} a_0 \ln f_i \tag{7a}$$

$$a_{iij} = \frac{s_{i,j} - 2s_{0,j} + s_{-i,j}}{2\alpha^2} a_0 \ln f_j \quad (i \neq j) \tag{7b}$$

In many cases, the curvature of η may be too large to be described by Eq. (1). A more suitable logarithmic response surface

$$\ln \eta = a_0 + \sum_i^L a_i x_i + \sum_i^L \sum_{j \geq i}^L a_{ij} x_i x_j + \sum_i^L \sum_{j \geq i}^L \sum_{k \geq j}^L a_{ijk} x_i x_j x_k \tag{8}$$

may be used. Following the SAB method, the polynomial coefficients are easily developed here as

$$a_0 = \ln \eta_0 \tag{9a}$$

$$a_i = \frac{\ln \eta[\mathbf{x}(\alpha)_i] - \ln \eta[\mathbf{x}(-\alpha)_i]}{2\alpha} \quad (i = 1, 2 \ldots, L) \tag{9b}$$

$$a_{ii} = \frac{s_{i,i} - s_{-i,i}}{4\alpha} \ln f_i \tag{9c}$$

$$a_{ij} = \frac{[(s_{i,j} - s_{-i,j}) \ln f_j + (s_{j,i} - s_{-j,i}) \ln f_i]}{4\alpha} \quad (i \neq j) \tag{9d}$$

The third-order terms are similarly determined by

$$a_{iii} = \frac{s_{i,i} - 2s_{0,i} + s_{-i,i}}{6\alpha^2} \ln f_i \tag{9e}$$

$$a_{iij} = \frac{s_{i,j} - 2s_{0,j} + s_{-i,j}}{2\alpha^2} \ln f_j \quad (i \neq j) \tag{9f}$$

Previous mechanism optimization studies [1,2,4–7] show that second-order polynomials are often sufficiently accurate. Here, since these partial third order terms are readily available, their effect on the accuracy of the response surface will be examined. For selected cases, three-way coupling $x_i x_j x_k$ terms are also examined. The coefficients of these terms are determined by calculating the second order "*ij*" terms at each of the x_k points and then finite differencing them with respect to k. This requires an additional $2L + 1$ local sensitivity calculations.

Gaseous Reacting Flow Simulations

The SAB method is applied to the modeling of the laminar flame speed, a fundamental property of hydrocarbon combustion [11]. The laminar flame speed is solved as an eigenvalue of a set of second-order, ordinary differential equations governing species and energy conservation with detail gas-phase reaction chemistry [12]. Aside from flame speed, we also test the SAB method for intermediate species concentration during fuel oxidation in a similar one-dimensional laminar combusting flow. Equation (1) is used to construct the response surfaces of flame speed, whereas logarithmic response surface, Eq. (8), is used for species concentration.

All gas-phase reacting flow simulations are performed with the Sandia ChemKin/PREMIX codes [13,14]. The PREMIX code is modified to automate the SAB procedure. The local sensitivity coefficients are computed in two ways. The first used the Jacobian matrix, **J**. The sensitivity coefficients are obtained by solving the linear system of equations

$$\mathbf{J}\frac{\partial \boldsymbol{\varphi}}{\partial \mathbf{k}} + \frac{\partial \mathbf{F}}{\partial \mathbf{k}} = 0 \tag{10}$$

where **F** is the residual vector of the discretized governing equations, $\boldsymbol{\varphi}$ is the solution vector (mass flux, temperature, and species mass fractions), and **k** is the parameter vector.

The sensitivity coefficients determined from the above approach are not as accurate as we had expected. The problem is related to the artificial boundary condition of free-flame anchoring or the TFIX [13] value. Table I shows the sensitivity coefficients calculated for the six most influential reactions on the H_2/CO flame speed. It is seen that the sensitivity coefficient values vary significantly as a function of TFIX. For this reason, we also obtain the sensitivity coefficients by numerically perturbing rate parameters and explicitly solving for the flame structure and speed. This method is hereafter referred to as the brute-force method. The perturbation is kept small (1.0×10^{-5}) so the sensitivity coefficient is local. Table I shows that the results from the brute force calculation are independent of the choice of TFIX value, as expected. Furthermore, the differences between the "small" perturbation factor (1.0×10^{-5}) and much more coarse perturbation factor (0.07) are negligibly small. For brute force calculations, only a few iterations are needed for Newton's convergence. Therefore, the method is only marginally more expensive than the Jacobian method.

Several computational methods are analyzed and compared with the factorial design method. Using the brute force (BF) sensitivity, we construct the response surfaces of the second (2BF), partially third (p3BF), and full third (f3BF) orders. The corresponding methods using the Jacobian-derived sensitivity are termed as 2J and p3J.

Four flames are studied, three of which are flame speed response surfaces that contain small, medium, and large number of active parameters. The first flame has an unburned mixture containing 80%H_2 and 20%CO, oxidized stoichiometrically in diluted air ($\{O_2\}/\{O_2+N_2\} = 11.7\%$) at 298 K and atmospheric pressure. The flame is hereafter referred to as the wet

Table I Comparison of the Sensitivity Coefficients Calculated for the Wet CO Flame Speed (80%H_2-20%CO in a Diluted Air of $[O_2]/[O_2 + N_2] = 11.7\%$ Under the Stoichiometric Condition, at 298 K and Atmospheric Pressure)

	Jacobian Sensitivity Coefficients				Brute Force Sensitivity Coefficients		
Reaction	300[a] –	400[a] –	800[a] –	1000[a] –	400[a] 1×10^{-5}[b]	1000[a] 1×10^{-5}[b]	400[a] 0.07[b]
1. $H + O_2 = O + OH$	0.122	0.144	0.169	0.181	0.168	0.168	0.168
2. $O + H_2 = H + OH$	0.125	0.148	0.174	0.177	0.173	0.173	0.172
3. $H_2 + OH = H_2O + H$	0.187	0.221	0.254	0.258	0.251	0.251	0.250
4. $H + O_2(+M) = HO_2(+M)$	−0.133	−0.157	−0.148	−0.129	−0.111	−0.111	−0.110
5. $HO_2 + H = 2OH$	0.160	0.190	0.213	0.214	0.209	0.210	0.208
6. $CO + OH = CO_2 + H$	0.157	0.186	0.215	0.223	0.208	0.208	0.207

[a] Represents value of TFIX in Kelvin.
[b] Represents the perturbation factor.

CO flame, and it has six active rate parameters. The parameter spans are purposely chosen to be larger than the true uncertainties so as to exaggerate the curvature of the response surface. The gas-phase H_2-CO reaction model and thermodynamic properties employed in the present study are taken from [15]. The second and the third cases are methane and propane flames, chosen from a recent study [7], and entail flame speeds of methane (10 active parameters) and propane (13 active parameters) at equivalence ratios of 0.98 and 1.2, respectively. The kinetic model used for the methane and propane flames consists of 70 species and 463 reactions [7]. The last case refers to the maximum O atom mole fraction in a burner-stabilized H_2-CO flame with conditions identical to the wet CO flame.

Surface Reaction Mechanism

Quantum mechanical techniques, and in particular density functional theory (DFT), are emerging as powerful tools for estimation of energetics. However, because of their computational cost, it is a daunting task to carry out on-the-fly calculation of activation energies or to apply DFT to large surface reaction mechanisms [2]. For this reason, semiempirical techniques are often more appropriate to estimate activation energies of elementary surface reactions [16]. These techniques include the unity bond index-quadratic exponential potential (UBI-QEP), known also as bond order conservation (BOC) [17,18] method. The inputs to UBI-QEP are heats of chemisorption of surface species, which are much more readily available or can easily be estimated. For the present study, the heats of chemisorption are summarized in Table II. The accuracy of the technique can be ±2–4 kcal/mol. An advantage of this approach is that coverage dependence in activation energies can be assessed, and thermodynamic consistency is assured. Large variations of the activation energy as a function of temperature (from catalyst ignition to flame temperatures) are predicted rather than tuned.

The accurate calculation of preexponential factors for supported or polycrystalline catalysts in nontrivial. Similar is the case with sticking coefficients. Experimental values, if known, can be used. Alternatively, classical transition state theory (TST) can provide order-of-magnitude estimates of preexponential factors. These estimates along with the activation energies at zero coverage are presented in Table III. Because of the difficulty in estimating preexponentials and their relatively small variation with conditions, we prefer to perform optimization of selected sticking coefficients and preexponentials. Use of solution mapping was proposed for this purpose in [8] and applied to hydrogen and carbon monoxide reactions on Pt [8,9]. These studies followed the same protocol developed in [1,4]. An interesting difference from the optimization of gas-phase combustion reaction mechanisms discussed above is that the uncertainty in these parameters is large (often 1–2 orders of magnitude for preexponentials and even larger for sticking coefficients).

Table II Heats of Chemisorption on Pt(111) Except Where Indicated

Species	Heat of Chemisorption (kcal/mol)	Reference	Comment
H	$60.2–4.8\theta_{H^*}$	[19]	
O	$92.6–25.6\theta_{O^*}$	[19]	
OH	$63.0–33.0\theta_{O^*}$	[16]	Polycrystalline Pt
H_2O	10.0	[20]	

θ indicates coverage of the surface species.

RESULTS AND DISCUSSION

Gaseous Reacting Flows

Here we demonstrate the applicability of the SAB method in gas-phase reacting flows, using vigorously burning flames. We start with the wet CO flame that yields a nominal flame speed of $s_u^\circ = 51.48$ cm/s. The active parameters are chosen from a sensitivity analysis, as shown in Table IV. In an initial test, the response surface coefficients are computed by the local first and second derivatives at the center point of the hypercube, i.e., by setting $\alpha \to 0$ in Eqs. (3) and (4). The resulting response surface is found to be inaccurate on the edge of the hypercube. In subsequent analyses, response surfaces of $\eta = s_u^\circ$ are constructed using finite α values (0.25, 0.50, and 0.75). The accuracy of the response surfaces is examined and compared using 200 random points within the hypercube as well as the 45 points used in the 2^{6-1} fractional factorial design (including the 6×2 star points outside the hypercube). The star points were used to ensure that the response surface works well on the edge of the uncertainty space. Results are summarized in Table V and shown in Fig. 2. One can immediately notice that there is only a small difference amongst the surfaces obtained with different α values. For this reason, all subsequent analyses are made using $\alpha = 0.5$.

Method 2BF produced a far more accurate response surface than the 2^{6-2} fractional factorial design and it performs similarly to the 2^{6-1} design. Within the hypercube the mean and RMS errors are 0.6 and 0.9 cm/s, respectively, and are smaller than the corresponding errors of 2^{6-1} design (0.8 and 1.0 cm/s). The maximum error of Method 2BF (5.2 cm/s) is, however, larger than

Table III Surface Reaction Mechanism of H_2 Oxidation on Polycrystalline Pt[a]

				Optimized Prefactor	
No.	Reaction	Trial Prefactor	Activation Energy	Method 2J	Factorial Design[c]
1	$H_2 + 2^* \rightarrow 2H^*$	1	0.0	1	1
2	$2H^* \rightarrow H_2 + 2^*$	1.0×10^{13}	20.0	1.0×10^{13}	1.0×10^{13}
3[b]	$O_2 + 2^* \rightarrow 2O^*$	0.1	0.0	2.7×10^{-1}	5.5×10^{-1}
4[b]	$2O^* \rightarrow O_2 + 2^*$	1.0×10^{13}	51.0	2.4×10^{14}	1.2×10^{14}
5	$OH^* + ^* \rightarrow H^* + O^*$	1.0×10^{11}	24.4	1.0×10^{11}	1.0×10^{11}
6	$H^* + O^* \rightarrow OH^* + ^*$	1.0×10^{11}	12.1	1.0×10^{11}	1.0×10^{11}
7[b]	$H_2O^* + ^* \rightarrow H^* + OH^*$	1.0×10^{11}	18.4	1.9×10^{11}	2.5×10^{11}
8	$H^* + OH^* \rightarrow H_2O^* + ^*$	1.0×10^{11}	12.4	1.0×10^{11}	1.0×10^{11}
9	$H_2O^* + O^* \rightarrow 2OH^*$	1.0×10^{11}	12.6	1.0×10^{11}	1.0×10^{11}
10	$2OH^* \rightarrow H_2O^* + O^*$	1.0×10^{11}	18.9	1.0×10^{11}	1.0×10^{11}
11[b]	$OH + ^* \rightarrow OH^*$	1	0.0	2.0×10^{-2}	2.0×10^{-2}
12[b]	$OH^* \rightarrow OH + ^*$	1.0×10^{13}	63.0	7.0×10^{13}	6.3×10^{13}
13[b]	$H_2O + ^* \rightarrow H_2O^*$	0.7	0.0	1.4×10^{-2}	6.9×10^{-3}
14[b]	$H_2O^* \rightarrow H_2O + ^*$	1.0×10^{13}	10.0	2.4×10^{14}	2.0×10^{14}
15	$H + ^* \rightarrow H^*$	1	0.0	1	1
16	$H^* \rightarrow H + ^*$	1.0×10^{13}	60.2	1.0×10^{13}	1.0×10^{13}
17	$O + ^* \rightarrow O^*$	1	0.0	1	1
18	$O^* \rightarrow O + ^*$	1.0×10^{13}	92.6	1.0×10^{13}	1.0×10^{13}

[a] The activation energies are in kcal/mol, calculated at zero coverage condition ($\theta_* = 1$). Prefactors refer to preexponentials in s^{-1} or sticking coefficients for adsorption steps (values less than or equal to 1). Note that these numbers, obtained only from LIF, differ from the manually fitted ones [16] or those rigorously optimized against multiple sets of experimental data in [8].

[b] Active prefactors that are optimized.

[c] Parameters obtained by full factorial design using a span of 2, starting from the optimum obtained using the SAB method after three iterations.

that of the factorial design (3.8 cm/s). The CPU requirement of the SAB method is only 1/10 of that of the 2^{6-1} design. Method 2BF also gives a more accurate response surface than the 2^{6-2} factorial design, and it needs 1/5 of the CPU time compared to the 2^{6-2} design.

We also wanted to evaluate if the accuracy of the response surface may be further improved by including

Table IV Active Rate Parameters for the Wet CO Flame Speed and Maximum in O Radical

	Sensitivity Coefficient (s)		
Reaction	Brute Force	Jacobian	Span (f)
Flame speed			
1. $H + O_2 = O + OH$	0.17	0.14	2.0
2. $O + H_2 = H + OH$	0.17	0.15	2.0
3. $H_2 + OH = H_2O + H$	0.25	0.22	2.0
4. $H + O_2(+M) = HO_2(+M)$	−0.11	−0.16	3.0
5. $HO_2 + H = 2OH$	0.21	0.19	3.0
6. $CO + OH = CO_2 + H$	0.21	0.19	2.0
Maximum in O radical			
1. $H + O_2 = O + OH$		0.11	2.0
2. $O + H_2 = H + OH$		−0.20	2.0
3. $H + OH + M = H_2O + M$		−0.05	2.0
4. $H + O_2(+M) = HO_2(+M)$		−0.28	3.0
5. $HO_2 + H = H_2 + O_2$		0.04	3.0
6. $HO_2 + H = 2OH$		−0.07	3.0
7. $CO + OH = CO_2 + H$		−0.05	2.0

Table V Comparison of CPUs and Absolute Errors (cm/s) of Response Surfaces for the Wet CO Flame (Nominal $s_u^\circ = 51.48$ cm/s)

Case	α	Number of Runs[a]	Relative CPU	200 Random Points			2^{6-1} Fraction Factorial Points[b]		
				Mean	RMS	Maximum	Mean	RMS	Maximum
SAB method									
2BF	1/4	13(S)	–	0.6	1.0	5.5	2.3	3.3	9.2
	1/2	13(S)	0.11	0.6	0.9	5.2	2.2	3.2	8.9
	3/4	13(S)	–	0.6	0.9	4.7	2.0	2.9	9.0
p3BF	1/4	13(S)	–	0.3	0.4	2.3	1.7	2.3	5.7
	1/2	13(S)	0.11	0.3	0.4	2.1	1.6	2.1	5.1
	3/4	13(S)	–	0.3	0.4	1.9	1.5	2.0	4.9
f3BF	1/2	13(S)	0.40	0.2	0.3	2.0	1.1	1.6	4.6
2J	1/2	13(S)	0.05	0.8	1.2	7.8	2.1	3.3	14.4
p2J	1/2	13(S)	0.05	0.7	0.9	4.1	1.7	2.3	6.6
Factorial design method									
2^{6-1}		45(F)	1.00	0.8	1.0	3.8	1.2	1.6	3.9
2^{6-2}		29(F)	0.55	1.4	1.9	8.3	2.9	4.8	18.2

[a] "F" denotes the number of flame calculation. "S" denotes the number of sensitivity runs.
[b] Star points in the analysis were included in the error analysis.

the partial third order x_i^3 and $x_i^2 x_j$ terms (Method p3BF). As noted earlier, the coefficients of these terms are obtained without having to perform additional computations. Table V and Fig. 2 show that Method p3BF is more accurate than 2BF and the factorial designs, especially in regions of the hypercube away from the corners where the $x_i x_j x_k$ $(i \neq j \neq k)$ terms are unimportant. Within the hypercube, the mean and maximum errors are 0.3 cm/s and 2.1 cm/s, respectively, both of which are notably smaller than those of the 2^{6-1} factorial design at 0.8 and 3.8 cm/s.

We also examine a response surface that includes all third order terms (f3BF) by invoking an additional $2L + 1$ sensitivity calculations, as discussed before. The accuracy is only slightly better than that using p3BF (see Table V and Fig. 2). The minor improvement, coupled with greater CPU requirements, does not warrant its use. A comparison is also made using the sensitivity coefficients calculated by methods 2J and p3J. It is seen that although these methods are less accurate than 2BF and p3BF, their CPU savings are even more significant.

Response surfaces of $\eta = s_u^\circ$ are constructed for the methane and propane flames. Table VI presents relative CPU times and the errors of various methods. Figure 3 shows the parity plots for the methane flame. Again, method 2BF gives an accuracy similar to the 2^{L-4} factorial design, but at a fraction of the cost. Specifically, it requires only 15 and 3% of the total CPU time of the 2^{L-4} factorial design for the methane and propane flames, respectively. Method 2J gives even greater CPU savings with the computational times reduced to 5% and 1% of the factorial method for the methane and propane flames, respectively. At the same time, the accuracy of the response surface is well preserved. For both flames, the mean and maximum errors of Method 2J are less or equal to 0.5 and 1 cm/s, respectively, which are well below finite differencing errors resulting from finite mesh resolution in the PREMIX solution. Little improvements are obtained with the use of the third order terms, as seen by comparing the accuracy of Methods 2BF and p3BF (see, Table VI).

To demonstrate that the SAB method is accurate and efficient for other combustion responses, a response surface is constructed for the O-atom concentration in a burner-stabilized wet CO flame. The response surface is given by $\eta = \ln(X_{\max})$, where $X_{\max}$ is the maximum mole fraction. Here, the local first-order sensitivity coefficients are computed using the Jacobian method. Figure 4 shows that the surfaces produced by Methods 2J and p3J are very accurate.

Lastly, we note that by using an automated computational code, we are able to obtain the response surface of a dozen or so rate parameters with similar CPU as what would be required for a normal sensitivity scan for all reaction rate parameters. Implementing and using the technique as a part of the sensitivity calculation makes the standard sensitivity analysis only marginally more expansive. The response surface, however, provides quantitative predictions for the response value without having to recompute the flame when rate parameters are adjusted. Thus even for the trial-and-error type of approach of reaction mechanism development, this is worthwhile.

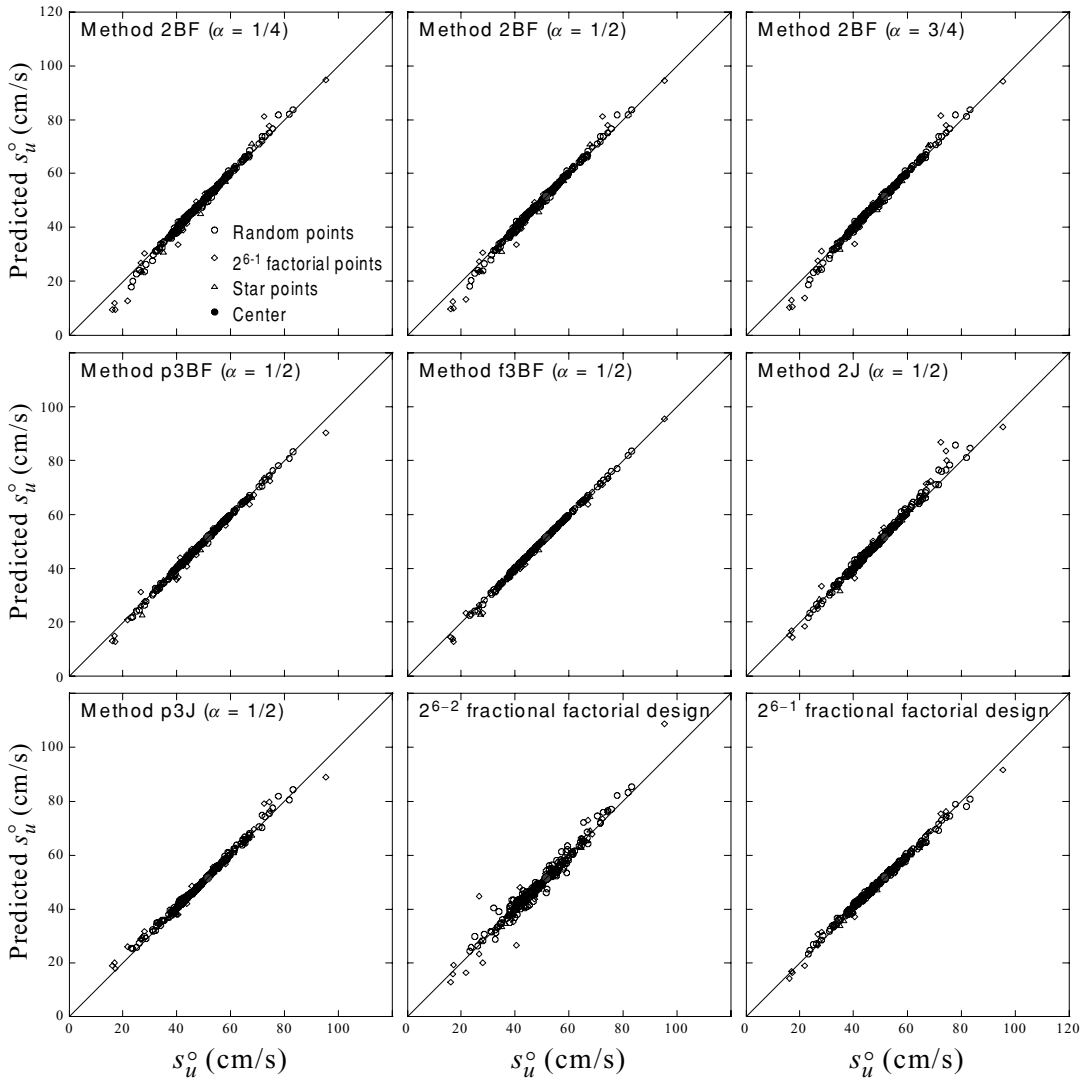

Figure 2 Response surface predictions for the wet CO flame versus direct numerical flame solutions.

A Prototype Example of Surface Reactions: Optimization of LIF Data

We focus on optimizing rate parameters of the H_2/O_2 reaction mechanism based on low pressure LIF data [21] with water and oxygen as reactants on a polycrystalline Pt foil. These experiments are among a few that provide information about the coupling of gas and surface chemistries, and motivate the particular choice.

Because of the low pressure and consequently large mean free path, the reactor is modeled as a continuous stirred tank reactor (CSTR). This is certainly a gross but common assumption [21]. The steady state equations for the surface coverage are solved using Newton's method. Figure 5 shows the poor prediction of the unoptimized model against the experimental data. Jacobian-based sensitivity analysis is an efficient and accurate method of choice for this problem. More details can be found in [22].

Figure 6 shows sensitivity analysis at extreme temperatures of the experimental data. For all temperatures analyzed (1111–1800 K), six active parameters are found, which include the sticking coefficients of O_2, OH, and H_2O and the desorption preexponentials of the same species. The selection of active parameters is made on the basis of a cut-off, normalized sensitivity value ranging from 0.01 to 0.04 at different temperatures. OH response surfaces of the six active parameters are obtained in an automatic way using both full 2^6 factorial design and the SAB method. For the latter method, values of α in the range 0.3–0.7 have a negligible effect on the accuracy of polynomials,

Table VI Comparison of CPUs and Absolute Errors (cm/s) of Response Surfaces for the Methane Flame (Nominal $s_u^\circ = 37.69$ cm/s) and Propane Flame (Nominal $s_u^\circ = 44.59$ cm/s)

Case	Number of Runs[a]	Relative CPU	50 Random Points			2^{L-4}Fraction Factorial Points[b]		
			Mean	RMS	Maximum	Mean	RMS	Maximum
Methane flame								
SAB method ($\alpha = 0.5$)								
2BF	21(S)	0.15	0.2	0.2	0.7	0.4	0.6	1.9
p3BF	21(S)	0.15	0.2	0.2	0.5	0.4	0.5	1.4
2J	21(S)	0.05	0.2	0.2	0.6	0.4	0.6	1.6
p3J	21(S)	0.05	0.2	0.2	0.5	0.3	0.4	1.0
Factorial design method								
2^{10-4}	85(F)	1.00	0.3	0.3	0.7	0.6	0.7	1.5
Propane flame								
SAB method ($\alpha = 0.5$)								
2BF	27(S)	0.03	0.2	0.2	0.7	0.6	0.8	3.8
p3BF	27(S)	0.03	0.2	0.2	0.7	0.6	0.8	3.3
2J	27(S)	0.01	0.6	0.6	1.0	0.7	0.9	4.6
p3J	27(S)	0.01	0.5	0.6	1.0	1.0	1.2	4.5
Factorial design method								
2^{13-4}	539(F)	1.00	0.3	0.3	0.9	0.4	0.6	3.1

[a] "F" denotes the number of flame calculations. "S" denotes the number of sensitivity runs.
[b] Star points in the analysis were included in the error analysis.

consistent with the results obtained for the gas-phase combustion problems discussed earlier. In subsequent analysis, a value of $\alpha = 0.5$ is used. In this case, full factorial design requires $2^6 + 2 \times 6 + 1 = 77$ numerical simulations, whereas the SAB method requires $2 \times 6 + 1 = 13$ sensitivity calculations. Computations show that the SAB method requires a factor of 3 to 4 less CPU than the factorial method.

To assess the error in the hypercube of parameter space, 200 random points are generated in the uncertainty hypercube space. The model response and the response surface predictions are compared in a parity plot (Fig. 7) for the full 2^L factorial design (top panel) and the SAB method with third order terms (bottom panel). In both panels, the open symbols correspond to all 18 rate parameters being randomly perturbed by up to a factor of 2 (in each direction), whereas the filled symbols are obtained when only the sensitive rate parameters (6) are randomly perturbed by up to a factor of 2. It is observed that the response surfaces developed by the SAB are almost as accurate as those of the full factorial design.

Using these response surfaces, the difference between the model response and the experimental data was minimized using simulated annealing [23]. Because of the large uncertainty in the initial estimates, it is expected that the response surfaces of catalytic kinetic models are developed far away from the optimum and their accuracy around the optimum may be limited. For this reason, refinement of the response surface is made through an iterative procedure. Given a tentatively optimized mechanism, a sensitivity analysis is performed and a new response surface is developed. This is followed by another optimization. The procedure is repeated until satisfactory convergence is achieved.

The results of successive optimizations are shown in Fig. 5. We found that three iterations provide improved accuracy and no significant gain is obtained with further iterations. For example, the percentage error at 1111 K decreases at each iteration from 5.01%, to 0.64%, and finally to 0.47%. Note that while six active parameters are chosen in the first iteration, one additional parameter becomes active in subsequent iterations. Therefore, a total of seven parameters are optimized in the last iteration. The optimized preexponential values from the last round of optimization are presented in Table III. Response surface was also constructed using the factorial design method. The optimization yields essentially the same result as the SAB method, as seen in Table III.

The iterative scheme appears to work very effectively and is highly recommended for cases where the uncertainty in active parameters is large. The ability of the iterative approach to activate/deactivate parameters around the optimal point in the parameter space further illustrates the effectiveness of the proposed procedure. The computational savings using SAB are significant,

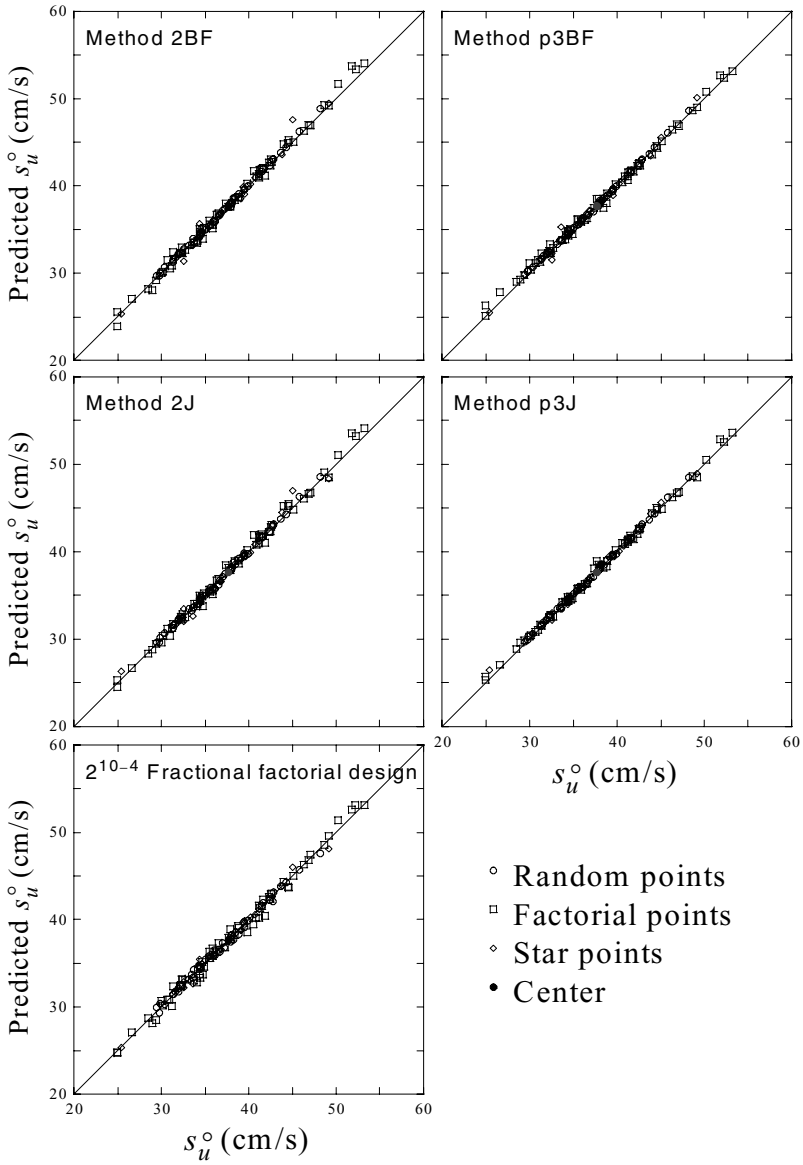

Figure 3 Response surface predictions for the methane flame versus direct numerical flame solutions.

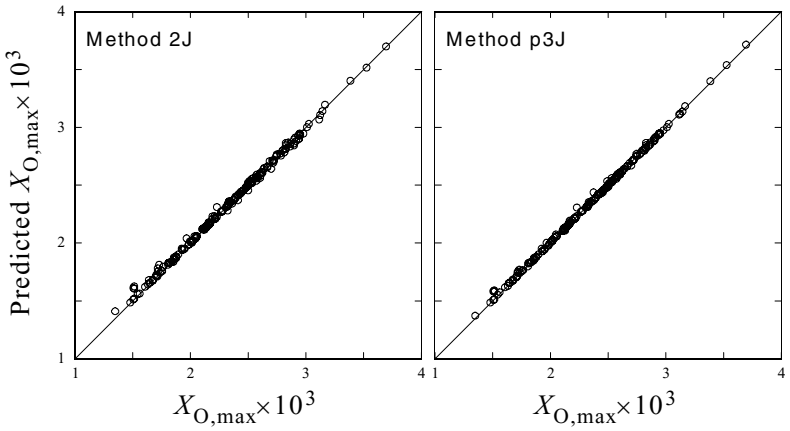

Figure 4 Response surface predictions of maximum mole fraction of the O atom for the burner-stabilized wet CO flame versus direct numerical flame solutions.

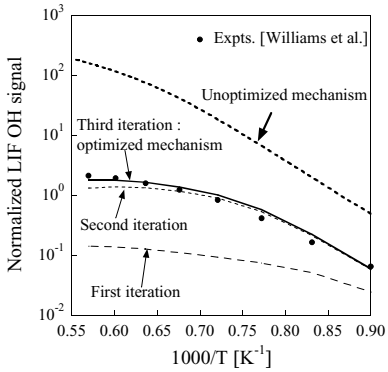

Figure 5 Experimental LIF data [19] and model predictions at various iterations of polynomial refinement versus inverse surface temperature. The conditions are reactor pressure of 0.2 Torr of H_2O and 0.3 Torr of O_2.

especially for expensive models containing many parameters. Further savings result when iterations are performed, as done above.

CONCLUSION

A new response surface method is developed for gas-phase and surface reaction model optimization. The SAB method proposed herein is derived from a multivariate Taylor expansion, and requires computation of first-order sensitivity coefficients. The application of the SAB method is demonstrated for four flames. It is found that the SAB method leads to a reduction of CPU usage by a factor of 10 or more. For heterogeneous surface reactions, optimization of some of the parameters of the H_2/O_2 surface reaction mechanism on Pt, using LIF experimental data, is demonstrated. Here local sensitivity analysis and an iterative solution mapping/optimization scheme are employed. Only a small number of iterations are needed to provide a converged kinetic scheme. A reduction in CPU usage by at least a factor of 3 has been observed, and more savings will result for larger problems. It is demonstrated that a response surface can be generated with computational demands similar to what would be required for a conventional local sensitivity analysis of all model parameters.

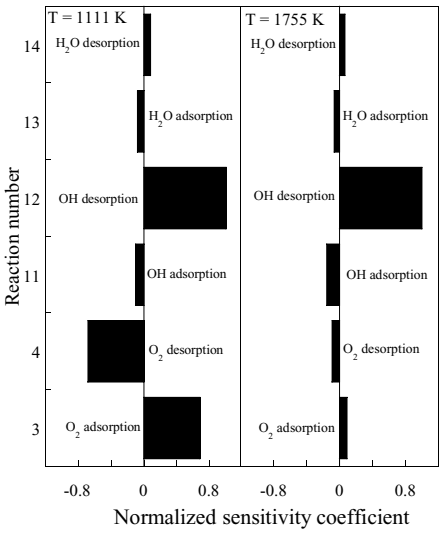

Figure 6 Normalized sensitivity analysis indicating the important steps in the unoptimized mechanism [8] at 1111 K and 1755 K. The rest of the parameters are the same as in Table III. In the whole range of temperature considered, adsorption and desorption of OH, O_2, and H_2O are the most important parameters.

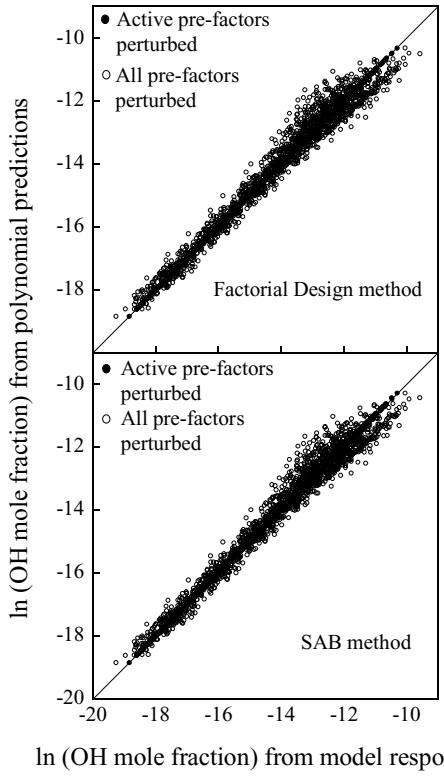

Figure 7 Natural logarithm of OH mole fraction predicted by response surfaces versus that obtained from direct simulation using the full model. The top panel corresponds to the complete factorial design method, whereas the bottom panel corresponds to the SAB method. In each panel, the open symbols correspond to all preexponentials perturbed randomly, whereas the filled symbols indicate random perturbation in the active preexponentials only.

The work is dedicated to the memory of Professor William C. Gardiner, Jr. The authors thank Professors William C.

Gardiner, Jr. and Fabian Mauss for helpful discussions. Any opinions, findings, conclusions, or recommendations expressed herein are those of the author(s) and do not necessarily reflect the views of the DOE.

BIBLIOGRAPHY

1. Frenklach, M.; Wang, H.; Rabinowitz, M. J. Prog Energy Combust Sci 1992, 18, 47.
2. Raimondeau, S.; Vlachos, D. G. Chem Eng J 2002, 90, 3.
3. Dumesic, J. A.; Rudd, D. F.; Aparicio, L. M.; Rekoske, J. E.; Trevino, A. A. The Microkinetics of Heterogeneous Catalysis; American Chemical Society: Washington, DC, 1993.
4. Frenklach, M. Combust Flame 1984, 58, 69.
5. Frenklach, M.; Wang, H.; Yu, C.-L.; Goldenberg, M.; Bowman, C. T.; Hanson, R. K.; Davidson, D. F.; Chang, E. J.; Smith, G. P.; Golden, D. M.; Gardiner, W. C.; Lissianski, V. Gas-Research-Institute mechanism for natural gas; taken from http://www.me.berkeley.edu/gri_mech/version12: 1996.
6. Smith, G. P.; Golden, D. M.; Frenklach, M.; Moriarty, N. W.; Eiteneer, B.; Goldenberg, M.; Bowman, C. T.; Hanson, R. K.; Song, S.; Gardiner, W. C. J.; Lissianski, V. V.; Qin, Z. GRI-mech 3.0: Gas-Research-Institute mechanism for natural gas; taken from http://www.me.berkeley.edu/gri_mech/: 2000.
7. Qin, Z.; Lissianski, V.; Yang, H. X.; Gardiner, W. C.; Davis, S. G.; Wang, H. Proc Comb Inst 2001, 28, 1663.
8. Aghalayam, P.; Park, Y. K.; Vlachos, D. G. AIChE J 2000, 46, 2017.
9. Aghalayam, P.; Park, Y. K.; Vlachos, D. G. Proc Comb Inst 2000, 28, 1331.
10. Box, G. E. P.; Hunter, W. G.; Hunter, J. S. Statistics for Experiments. An Introduction to Design, Data Analysis, and Model Building; Wiley: New York, 1978.
11. Glassman, I. Combustion; Academic Press: San Diego, 1996.
12. Miller, J. A.; Kee, R. J.; Westbrook, C. K. Annu Rev Phys Chem 1990, 41, 345.
13. Kee, R. J.; Grcar, J. F.; Smooke, M. D.; Miller, J. A. A FORTRAN Program for Modeling Steady Laminar One-dimensional Premixed Flames; Sandia Report SAND85-8240 UC4: Albuquerque, NM, 1985.
14. Kee, R. J.; Rupley, F. M.; Miller, J. A. Chemkin-II: A FORTRAN Chemical Kinetics Package for the Analysis of Gas Phase Chemical Kinetics; Sandia National Laboratories Report, SAND89-8009: Livermore, CA, 1991.
15. Mueller, J. A.; Kim, T. J.; Yetter, R. A.; Dryer, F. L. Int J Chem Kinet 1999, 31, 113.
16. Park, Y. K.; Aghalayam, P.; Vlachos, D. G. J Phys Chem A 1999, 103, 8101.
17. Shustorovich, E. Adv Catal 1990, 37, 101.
18. Shustorovich, E.; Sellers, H. Surf Sci Rep 1998, 31, 1.
19. Shustorovich, E. Adv Catal 1990, 37, 101.
20. Shustorovich, E.; Bell, A. T. Surf Sci 1991, 248, 359.
21. Williams, W. R.; Marks, C. M.; Schmidt, L. D. J Phys Chem 1992, 96, 5922.
22. Tomlin, A. S.; Turanyi, T.; Pilling, M. J. Elsevier Sci J 1997, 35, 293.
23. Kirkpatrick, S.; Gelatt, C. D., Jr.; Vecchi, M. P. Science 1983, 220, 671.